

New Low-Cost Five-Level Active Neutral-Point Clamped Converter

Hongliang Wang, *Senior Member, IEEE*, Lei Kou,
Yan-Fei Liu, *Fellow, IEEE* and Paresh C. Sen, *Life
Fellow, IEEE*

Department of Electrical and Computer Engineering
Queen's University
Kingston, Canada

hongliang.wang@queensu.ca, kou.lei@queensu.ca,
yanfei.liu@queensu.ca, senp@queensu.ca

Abstract—Multilevel converters are a popular solution for medium-voltage and high-power applications, including renewable energy conversion. Five-level active neutral-point-clamped converter (5L-ANPC) is one of the most advantageous topologies among five-level multilevel converters. A six-switch 5L-ANPC (6S-5L-ANPC) topology is proposed, which can achieve low-cost because several fast recovery diodes are employed to replace the body-diodes and active switches. However, the power branches including the diode can only provide active current path. Special modulation strategy is proposed to achieve reactive power operation. The simulation analysis shows the proposed 6S-5L-ANPC is suitable for unity power factor application such as photovoltaic (PV) application. A 500W single-phase inverter prototype is built to verify the validity and flexibility of proposed topology and modulation.

I. INTRODUCTION

Multilevel converters (or inverters) have been used for power conversion in high-power applications such as medium voltage grid (2.3KV, 3.3KV, or 6.9KV) to reduce the switch voltage stress, and photovoltaic (PV) application to reduce the filter size [1, 2]. Compared to two-level voltage source inverters, the advantages of multilevel inverters are lower voltage stress, higher efficiency, smaller filter size and lower common-mode voltage [3].

There are three traditional multilevel topologies [4-8]: the neutral-point-clamped (NPC) type [4, 5], flying-capacitor (FC) type [6], and cascaded H-bridge (CHB) type [7-8]. Many five-level NPC topology has been derived in [9]. NPC

Sucheng Liu
School of Electrical and Information Engineering
Anhui University of Technology
Ma'anshan, China
liusucheng@gmail.com

type generates the voltage levels from the neutral point voltage by adopting diodes. The drawback is the increased number of switching devices when voltage level increases. FC type outputs the voltage level by summing the flying-capacitor voltage. However, higher voltage level leads to more flying-capacitors and the complexity of control strategy to balance the voltages of each flying-capacitor is then increased. The CHB multilevel inverters use series-connected H-bridge cells with an isolated dc voltage sources connected to each cell [10]. Similarly, to have more output levels, more cells are needed. This will lead to impracticality of this type of topology since more DC sources are required.

Active-neutral-point-clamped (ANPC) which is one of the multilevel topology has been proposed in Refs [11-15]. Three 5L-ANPC topologies are shown in Fig.1. The ANPC type converter combines the features of NPC and FC topology. The ANPC topologies is receiving more and more attentions nowadays because of high efficiency and multilevel output. In this paper, a novel six-switch five-level ANPC (6S-5L-ANPC) inverter topology is proposed. Compared to traditional ANPC topologies, the proposed topology adopts only six active semiconductor switches, greatly reducing the volume of system. This paper is organized as follows: Section II describes working principles of proposed topology; Section III discusses the modulation strategy of 6S-5L-ANPC topologies; Section IV and V show the simulation and experimental results and Section VI gives the conclusion.

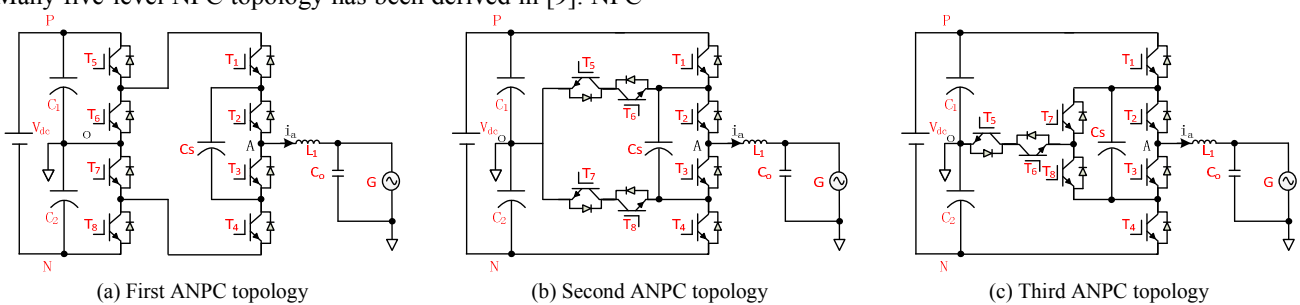


Fig. 1. Five-level ANPC topology

II. OPERATIONAL PRINCIPLES OF PROPOSED 6S-5L-ANPC INVERTER

A. Introduction of 6S-5L-ANPC Inverter

To increase the overall efficiency and improved output waveform, the five-level ANPC inverters are good choice for renewable energy harvesting. Additionally, based on half-bridge, the 5L-ANPC inverters guarantee no leakage current generation. Therefore, they are suitable for transformer-less type photovoltaic (PV) system. For grid-connection application, the inverter output current is required to be in phase with grid voltage. In this situation, reactive current paths can be ignored, which means some active switches can be replaced by fast recovery diodes in order to increase the efficiency. Based on this, a novel 5L-ANPC inverter topology is proposed, which is composed of six switches (T_1 to T_6), two discrete-diodes (D_{F1} , D_{F2}) and one flying-capacitor (C_s). The configuration of six-switch 5L-ANPC (6S-5L-ANPC) inverter is shown in Fig.2.

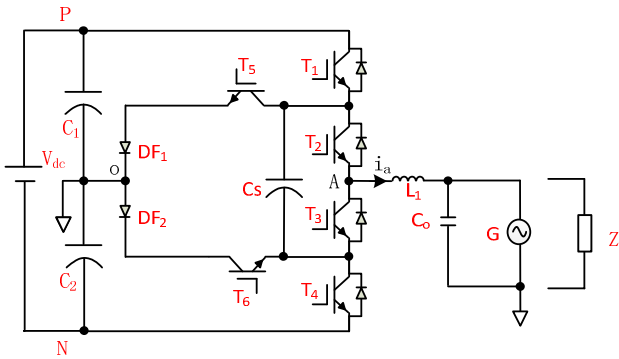


Fig. 2. Configuration of 6S-5L-ANPC inverter

As can be seen from Fig.2, two DC capacitors, C_1 and C_2 , are connected in series to DC-link. The complexity of DC-link capacitor voltages balancing is reduced compared to NPC and FC type converters which need four DC capacitors in series. Additionally, in contrast to traditional 5L-ANPC topologies (as shown in Fig.1) which need eight active switches and other types of five-level inverters which require

more, the proposed 6S-5L-ANPC inverter only has six active switches and two discrete diodes. The reduced number of active switches sacrifice some reactive current paths. However, the proposed topology is capable of operating under reactive power condition with special modulation method, which will be discussed in the following section.

B. Operation of 6S-5L-ANPC Topology

DC voltage is defined as V_{dc} . The 6S-5L-ANPC converter consists of eight switching states that generate five-level voltage levels at the output based on capacitor voltages (DC voltage and FC voltage), as shown in Table I. Five output voltage levels $+V_{dc}/2$, $+V_{dc}/4$, 0, $-V_{dc}/4$ and $-V_{dc}/2$ are achieved by summing the flying-capacitor voltage and DC-link capacitor voltage. Fig.3 shows the specific eight switching states (mode A to H) and current paths (active power branch in red line and reactive power branch in green line).

In Table I, it is observed that some of the switching states are redundant in generating certain output voltage level: mode B and mode C are redundant switching states to generate $+V_{dc}/2$; similarly, (D, E) and (F, G) are redundant states to generate 0 and $-V_{dc}/2$, respectively. Although the redundant states (B, C) and (F, G) generate the same output voltage level, their effect on the FC voltage is opposite to each other due to the change in the direction of FC current. This leads to the possibility of regulating the FC voltage to a constant value ($V_{dc}/4$).

In Fig.3, it is observed that among eight switching states, four modes (C, D, E, F) allow unidirectional current-flow path due to the presence of discrete diode. Therefore, appropriate selection of switching states under reactive power operation is very important, which also increases the complexity of modulation. Therefore, the proposed 6S-5L-ANPC converter is suitable for active power application (e.g. PV grid-connection application). The following section will cover the specific modulation strategy for proposed topology.

TABLE I. SWITCHING STATES, OUTPUT VOLTAGE AND VOLTAGE OF FLYING-CAPACITOR OF 6S-5L-ANPC INVERTER

Switching state	Switch number						Output voltage V_{AO}	Flying capacitor C_s	
	T_1	T_2	T_3	T_4	T_5	T_6		$i_a > 0$	$i_a < 0$
A	1	1	0	0	0	1	$+V_{dc}/2$	--	--
B	1	0	1	0	0	1	$+V_{dc}/4$	Charge	Discharge
C	0	1	0	0	0	1	$+V_{dc}/4$	Discharge	Charge
D	0	0	1	0	0	1	+0	--	--
E	0	1	0	0	1	0	-0	--	--
F	0	0	1	0	1	0	$-V_{dc}/4$	Discharge	Charge
G	0	1	0	1	1	0	$-V_{dc}/4$	Charge	Discharge
H	0	0	1	1	1	0	$-V_{dc}/2$	--	--

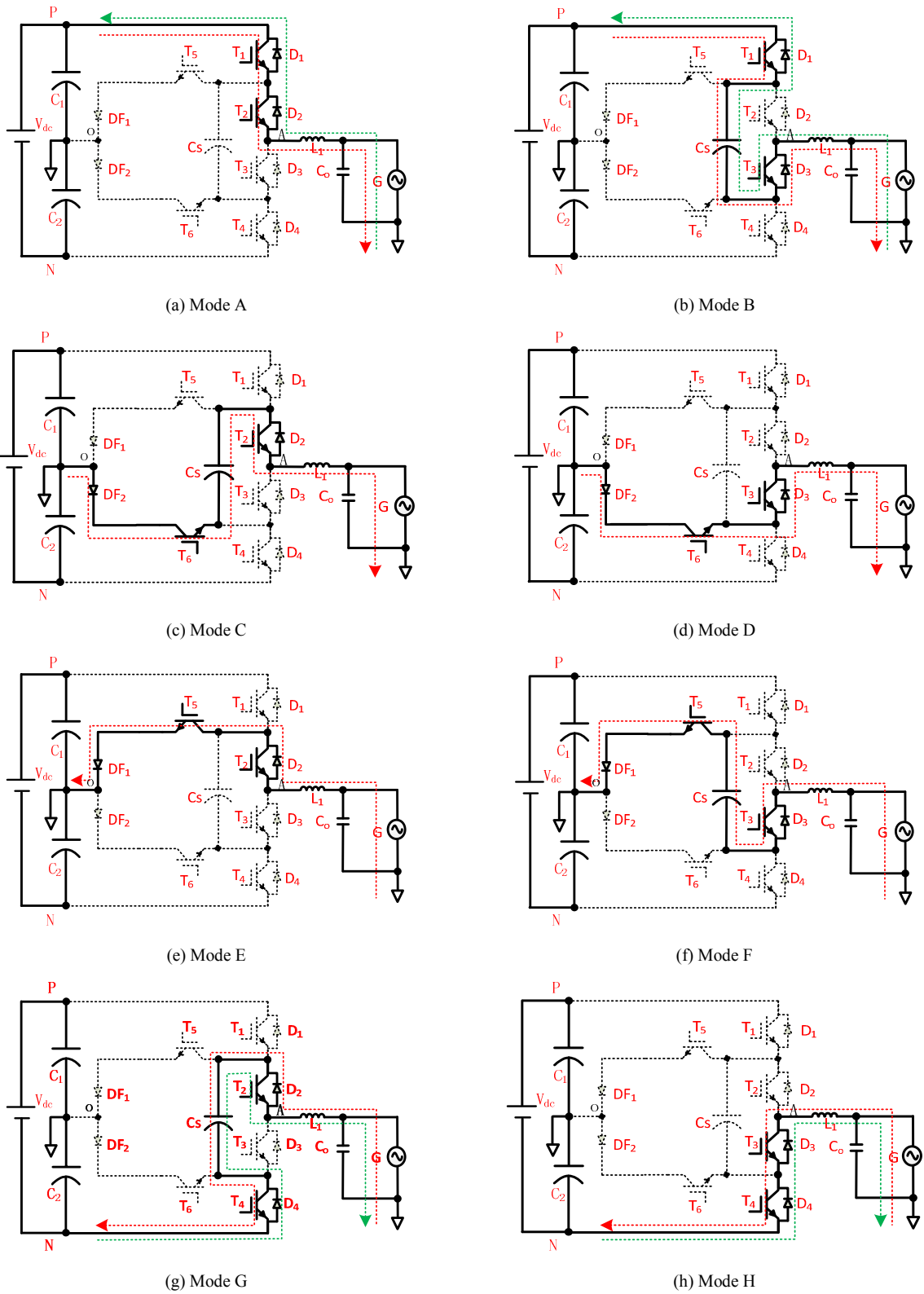


Fig. 3. Eight switching modes and current paths for 6S-5L-ANPC

III. MODULATION STRATEGY

As can be seen from Fig.3, four switching modes allow unidirectional current path due to the adoption of fast recovery diode. Therefore, the modulation method for 6S-5L-ANPC inverter is different from traditional ANPC topologies.

Selection of zero output states: both zero output modes (D and E) belong to unidirectional current path states: the current in mode D can only flow from left to right (positive) while mode E allows only negative current. So selection of zero output states is based on the direction of output current.

Among two pairs of redundant states which output $V_{dc}/2$ level, mode C ($+V_{dc}/2$) and F ($-V_{dc}/2$) allow unidirectional current-flow path. These two states can only be used when output voltage and current are in same direction. Therefore,

under reactive power factor condition, when directions of current and voltage are different, we can only use mode B ($+V_{dc}/2$) and E ($-V_{dc}/2$) to achieve $V_{dc}/2$ output level. This will result in the continuous drop of flying-capacitor voltage because both two modes are discharging the flying-capacitor. Consequently, if power factor is low which leads to wide region of output current and voltage in opposite direction, a large flying-capacitor voltage ripple will be generated. In this case, a large value of flying-capacitor is selected to reduce the voltage ripple.

From the analysis above, it is concluded that the complexity of modulation is increased when inverter is working under reactive power condition. Therefore, only reactive power modulation strategy is discussed. The diagram of modulation for 6S-5L-ANPC inverter is shown in Fig.4.

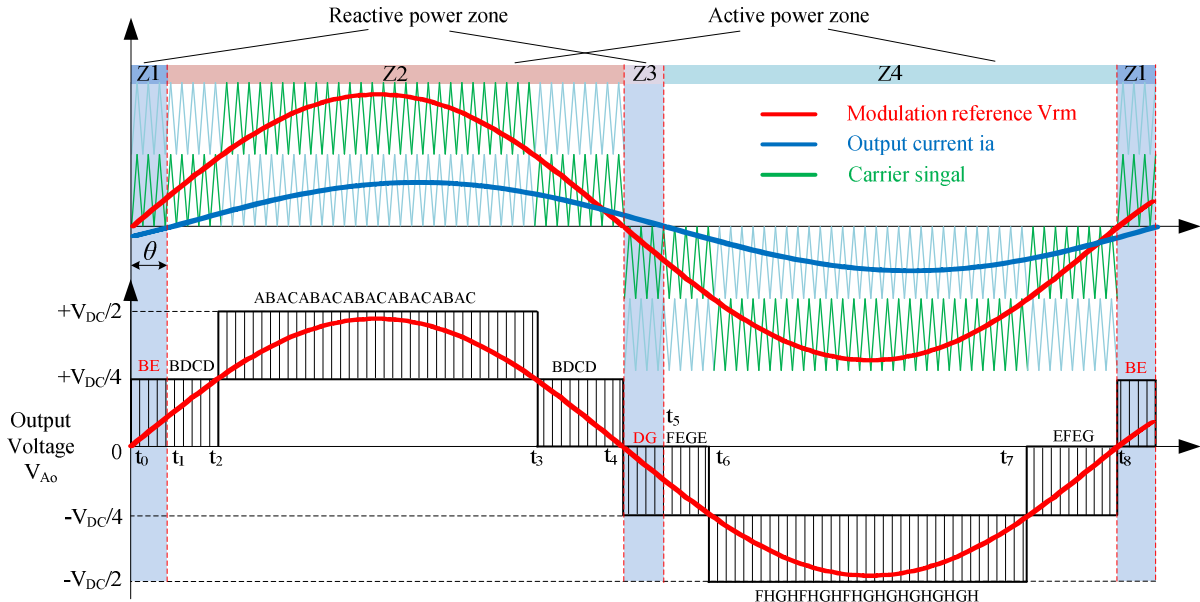


Fig. 4. PWM modulation for 6S-5L-ANPC inverter ($\cos\theta > \sqrt{3}/2$)

From Fig.4, it can be observed that during a whole grid cycle, there are four zones according to whether the output current and voltage are in same direction: Z1 and Z3 are reactive power zones while Z2 and Z4 are active power zones.

As mentioned before, the selection of two redundant switching states generation zero output is based on the direction of output current. So from t_1 to t_5 , the current is positive and mode D is chosen. Similarly, from t_0 to t_1 and t_5 to t_8 , mode E is selected due to the negative output current.

Reactive power zone Z1 [from t_0 to t_1]: inverter is outputting zero and $+V_{dc}/4$. In this region, only mode B can be used to generate $+V_{dc}/4$ output because voltage and current are in opposite direction. For zero output, mode E is

selected due the negative current. So, (B, E) states combination is obtained.

Active power zone Z2 [From t_1 to t_2 and t_3 to t_4]: the output voltage is switched between zero and $+V_{dc}/4$. Because it is in the active power zone, two redundant $+V_{dc}/4$ states can be used. This gives an opportunity to regulate the voltage across flying-capacitor. When actual FC voltage is lower than reference FC voltage, charging state B is chosen; when greater than reference FC voltage, mode C is selected to discharge flying-capacitor. When outputting zero voltage level, mode D is chosen. Consequently, the switching state sequence of (B, D, C, D) is achieved.

[From t_2 to t_3]: the output reference voltage is between $+V_{dc}/4$ and $+V_{dc}/2$. Mode A is required to generate $+V_{dc}/2$ output level. Similarly, in active power zone, appropriate

selection of redundant switching states (B, C) is necessary. In this way, sequence of (B, A, C, A) guarantees flying-capacitor voltage balancing and inverter output.

Reactive power zone Z3 [from t_4 to t_5]: output current is negative, so mode D is needed to output zero level. Mode G is selected to generate $-V_{dc}/4$ output. In this region, switching states sequence (D, G) is acquired.

Active power zone Z4 [From t_5 to t_8]: similar to zone Z2, mode D and mode H are selected for zero and $-V_{dc}/2$ output levels. When outputting $-V_{dc}/4$ voltage levels, redundant switching states (F, G) are employed alternately to keep flying-capacitor balanced. Consequently, during t_5 to t_6 and t_7 to t_8 , switching state sequence (F, E, G, E) is achieved; from t_6 to t_7 , switching state sequence (F, H, G, H) is adopted.

According the description of modulation strategy for 6S-5L-ANPC inverter topology, it is obtained that in reactive power zone, the flying-capacitor cannot be regulated. A higher value of flying-capacitor can be adopted in low power factor case. In conclusion, the proposed 6S-5L-ANPC inverter is suitable for active power application (e.g. PV grid-connection) and high power factor application.

IV. SIMULATION VERIFICATION

In order to testify the effectiveness of modulation strategy especially under reactive power condition, simulation verification has been carried out using MATLAB/Simulink. The simulation has been done in two cases: unity power factor operation and reactive power case. The power level of inverter system in the simulation is 500W. The system parameters are shown in Table II.

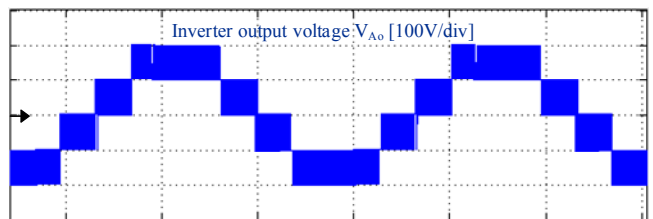
TABLE II. SYSTEM PARAMETERS

Input voltage	400V	Grid voltage	110V RMS
DC capacitor	$2000\mu F$	Grid frequency	60Hz
Flying capacitor	$310\mu F$	Output current	4.6A RMS
Output filter inductor	1.6mH	Switching frequency	15kHz

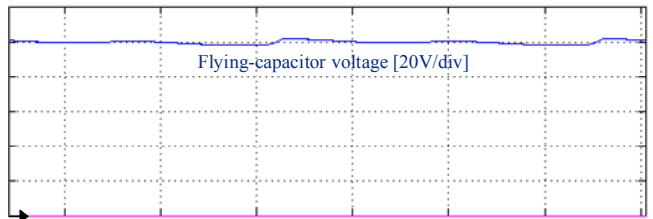
A. Unity power factor operation

To investigate the effectiveness of proposed topology and modulator, waveforms of inverter output voltage V_{Ao} , flying-capacitor voltage, grid voltage and output current are obtained from simulation, as shown in Fig.5.

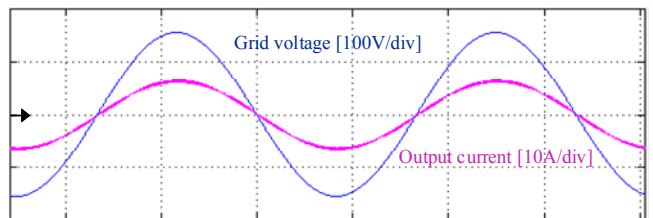
Fig.5 (a) shows the five-level inverter output. Fig.5 (b) shows the flying-capacitor voltage. From calculation, $310\mu F$ is chosen for flying-capacitor value. As can be seen, the FC voltage is kept at 100 volts, and 2 volts voltage variation is applied on the flying-capacitor. So voltage ripple in this case is 2%. Fig.5 (c) shows the gird-voltage and inverter output current. Under unity power factor, the current and voltage are in phase. The output current is sinusoidal wave without distortion.



(a)Inverter output voltage waveform



(b)Flying capacitor voltage waveform



(c)Grid voltage and output current waveform

Fig. 5. Active power operation: simulation waveforms of inverter output voltage, flying-capacitor voltage, grid voltage, output current

B. Reactive Power operation ($\cos\theta = 0.9$)

To verify the proposed modulation method in section III, simulation under high power factor case ($\cos\theta = 0.9$) has been carried out. Waveforms of inverter output voltage V_{Ao} , flying-capacitor voltage, grid voltage and output current are obtained from simulation are shown in Fig.5.

Compared to the output voltage in Fig.5 (a), the output voltage under reactive power condition is almost the same. As can be seen from Fig. 6 (a), a small voltage spike happens near the output current zero-crossing point. This is due to the switching states transition: the output current is changing from mode D to E (or from mode E to D).

In Fig.6 (b), it is observed that flying-capacitor voltage ripple is increased compared to unity power factor case. As can be seen, the large voltage ripples occur at reactive power zone (in Fig. 6 (c), the region where grid voltage and output current are in opposite direction). The waveform of FC voltage verify the analysis in section III: the FC voltage cannot be regulated in reactive power zone. Appropriate selection of flying-capacitor value can keep the voltage ripple within acceptable range. In my case, power level is 500W (input voltage is 400V and output current is 4.6A RMS) and $310\mu F$ flying-capacitor is selected to achieve maximum 6 volts (6%) ripple voltage.

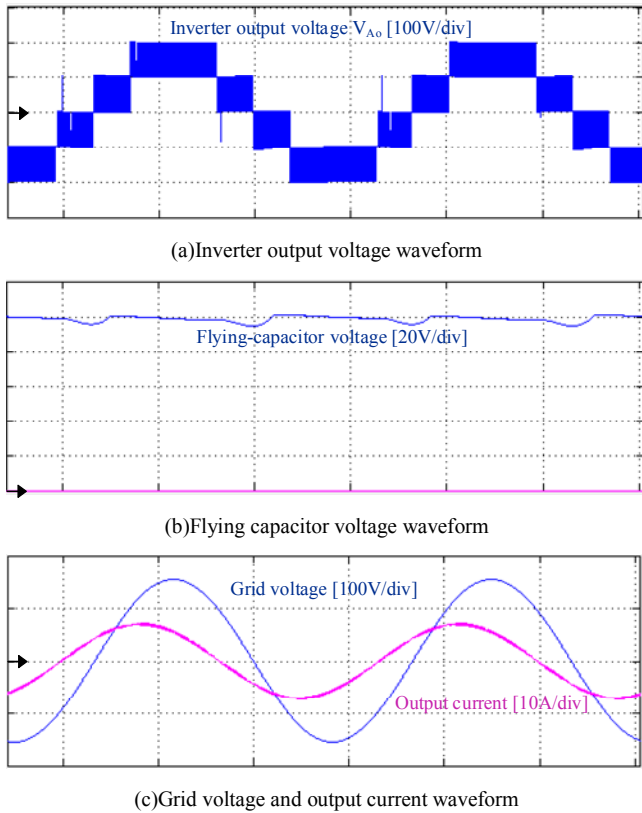


Fig. 6. Reactive power operation $\cos\theta = 0.9$: simulation waveforms of inverter output voltage, flying-capacitor voltage, grid voltage and output current

From the simulation results in two cases, it can be concluded that with proposed modulation method applied on proposed 6S-5L-ANPC inverter, the system is capable of operating under both active power condition and reactive power condition.

V. EXPERIMENTAL RESULTS

To verify the effectiveness of proposed topology and its modulation strategy. A 500W single-phase 6S-5L-ANPC inverter grid-connection experimental prototype is implemented, as shown in Fig.7. The system includes main circuit, DSP and FPGA control board, DC source, output filter and measurement instruments.

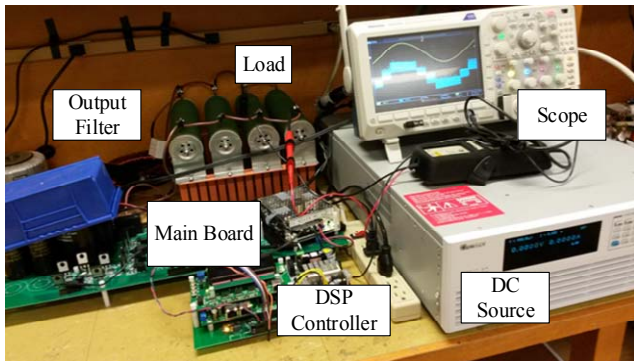


Fig. 7. Experimental prototype

The control board employs a combination of the Texas Instruments TMS320F28335 control card and the Altera Cyclone IV EP4CGX22 FPGA card to provide powerful real-time mathematical calculations and control functions. The experimental parameters are the same as parameters used in simulation, shown in Table II.

Fig.8 and Fig.9 show the experimental results under unity power factor condition. Fig.8 shows inverter output voltage, flying-capacitor voltage, grid voltage and output current: channel 1 is the output bridge voltage; channel 2 is 110V_{rms} grid voltage; channel 3 is the flying-capacitor voltage, which is balanced at 100 volts; channel 4 is the output current, which is sinusoidal without distortion and in phase with grid voltage in this case. Fig.9 shows two DC-link capacitors voltages, flying-capacitor voltage and output current: channel 1 is lower DC-link capacitor voltage and channel 2 is upper DC-link capacitor voltage, which both have a line-frequency fluctuation. The measured flying-capacitor ripple voltage is 3V (3%) and DC-link capacitor ripple voltage is 8V (4%).

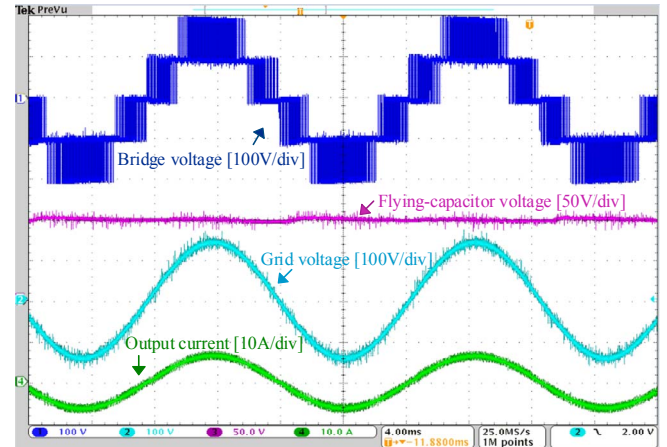


Fig. 8. Experimental results under unity power factor condition: waveforms of inverter bridge voltage, flying-capacitor voltage, grid voltage and output current

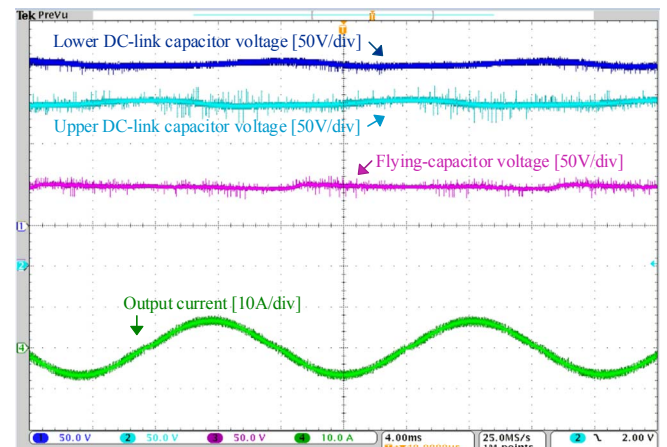


Fig. 9. Experimental results under unity power factor condition: waveforms of lower DC-link capacitor voltage, upper DC-link capacitor voltage, flying-capacitor voltage and output current

To testify the proper system operation under reactive power condition, experimental works are carried out. The power factor is selected as $\cos\theta = 0.9$. Fig.10, Fig.11 and Fig.12 show the experimental results.

Fig.10 shows inverter output voltage, flying-capacitor voltage, grid voltage and output current. It is observed that the waveform of inverter output voltage V_{AO} is same as one achieved in the simulation: small voltage spikes occur around output current zero-crossing points. The flying-capacitor voltage is also balanced at 100 volts. Under 0.9 power factor, the output current and grid voltage has a 25 degree phase shift. In this situation, the inverter still produces good quality current waveform without distortion.

Fig.11 shows two DC-link capacitors voltages, flying-capacitor voltage and output current. The DC-link capacitors voltages waveforms in this situation are almost the same as one under active power condition. The measured DC-link capacitor ripple voltage is also 8V (4%).

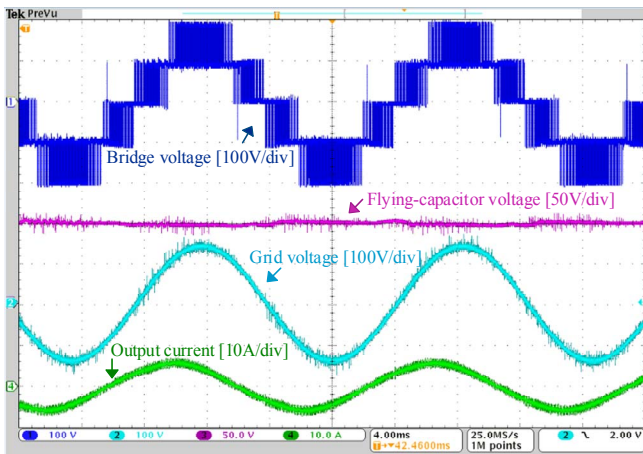


Fig. 10. Experimental results under reactive power operation $\cos\theta = 0.9$: waveforms of inverter bridge voltage, flying-capacitor voltage, grid voltage and output current

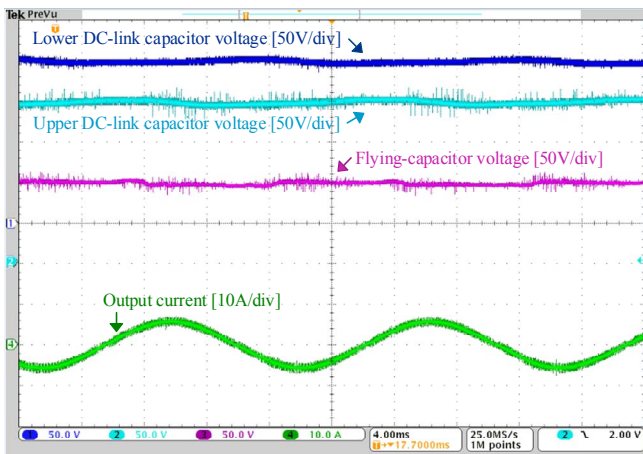


Fig. 11. Experimental results under unity power factor $\cos\theta = 0.9$: waveforms of lower DC-link capacitor voltage, upper DC-link capacitor voltage, flying-capacitor voltage and output current

Fig.12 shows lower DC-link capacitor voltage, flying-capacitor voltage, grid voltage and output current. It can be seen that large FC voltage ripple happen during the time when grid voltage and output current are in opposite direction. The voltage drop in reactive power zone is 7 volts (7%). The experimental results are consistent with analysis in section III and simulation results in section IV.

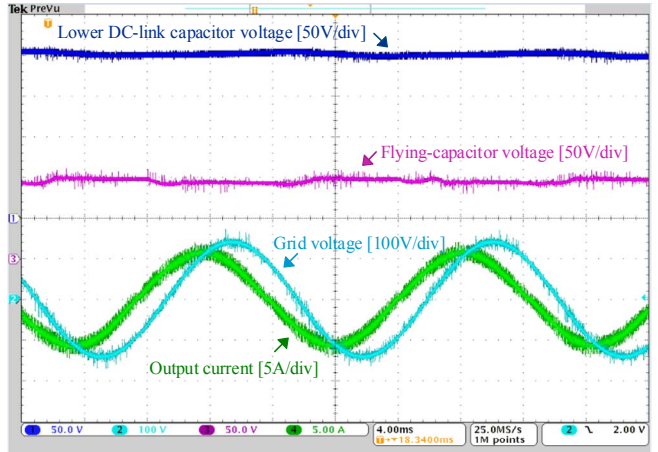


Fig. 12. Experimental results under unity power factor $\cos\theta = 0.9$: waveforms of lower DC-link capacitor voltage, flying-capacitor voltage, grid voltage and output current

VI. CONCLUSION

A novel six-switch five-level flying-capacitor based ANPC converter has been proposed. Compared to traditional 5L-ANPC converters, it reduces two active semiconductor switches. The working principles and switching states are presented. The specific modulation strategy of 6S-5L-ANPC inverter under reactive power operation has been investigated. Issues related to the balancing of flying-capacitor voltage and reactive power operation are discussed. The simulation and experimental verifications have been carried out in unity power factor condition and reactive power case to demonstrate the effectiveness of proposed topology and modulation method.

REFERENCE

- [1] P. Hammond. A New Approach to Enhance Power Quality for Medium Voltage AC Drives. *IEEE Trans. on Industry Applications*, 1997, 33(1): 202-208.
- [2] G. Beinholt, R. Jakob and M. Nahrstaedt. A New Range of Medium Voltage Multilevel Inverter Drives with Floating Capacitor Technology[C]. In: Conference Proceedings of the 9th European Conference on Power Electronics, EPE 2001, Austria, CD-ROM.
- [3] J. Rodriguez, J. S. Lai, and F. Z. Peng, "Multilevel inverters: A survey of topologies, controls, and applications," *IEEE Trans. Ind. Electron.* Vol. 49, no. 4, pp. 724–738, Aug. 2002.
- [4] A. Nabae, I. Takahashi, and H. Akagi, "A new neutral-point clamped PWM inverter," *IEEE Trans. Ind. Applicat.*, vol. IA-17, pp. 518–523, Sept./Oct. 1981.
- [5] J. Rodriguez, S. Bernet, B. Wu, J. O. Pontt, and S. Kouro, "Multilevel voltage-source-converter topologies for industrial medium-voltage drives," *IEEE Trans. Ind. Electron.*, vol. 54, no. 6, pp. 2930–2945, Dec. 2007.

- [6] F. Richardeau, P. Baudesson, and T. A. Meynard, "Failure-tolerance and remedial strategies of a PWM multi-cell inverter," *IEEE Trans. Power Electron.*, vol. 17, no. 6, pp. 905–912, Nov. 2002.
- [7] J. I. Leon, S. Kouro, S. Vazquez, R. Portillo, L. G. Franquelo, J. M.Carrasco, and J. Rodriguez, "Multidimensional modulation technique for cascaded multilevel converters," *IEEE Trans. Ind. Electron.*, vol. 58, no. 2,pp. 412–420, Feb. 2011.
- [8] Kagarlu,M.F and Babaei.E" A Generalized Cascaded Multilevel Inverter Using Series Connection of Sub-multilevel Inverters," *IEEE Trans. Power Electron.* Vol. 28, no. 2, pp. 625–636, Aug. 2013.
- [9] H. Wang, Y.-F. Liu, and P. C. Sen, "A neutral point clamped multilevel topology flow graph and space NPC multilevel topology," in Energy Conversion Congress and Exposition (ECCE), 2015 IEEE, 2015, pp. 3615-3621.
- [10] Kouro, S., Malinowski, M., Gopakumar, K., Pou, J., Franquelo, L., "Recent Advances and Industrial Applications of Multilevel Converters," *IEEE Trans. Ind. Electron.*, vol. 57, no. 8,pp. 2553-2580, Feb. 2010.
- [11] P.Barbosa, P. Steimer, J. Steinke, J. meysenc, "Active Neutral-point-clamped Multilevel Converter" *Power Electronics Specialists Conference, 2005. PESC' 05. IEEE 36th 16-16 June 2005.* (2001), 2001, pp. 2296-2301.
- [12] T. Brückner, S. Bernet, and H. Güldner, "The active NPC converter and its loss-balancing control," *IEEE Trans. Ind. Electron.*, vol. 52, no. 3, pp. 855–868, 2005.
- [13] L.A. Spepa, P.M. Brbosa, P.K. Steimer, and J. W. Kolar, "Five-Level virtual -flux direct power control for the active neutral-point-clamped multilevel inverter," in Proc. IEEE PESC, Jun. 2008, PP. 1668-1674.
- [14] K.Wang, Y.Li and Z. Zheng, "A neutral-point potential balancing algorithm for five-level ANPC converters," in Proc. ICEMS, Aug. 2011, pp. 1-5.
- [15] Soeiro.T.B, Carballo. R, Moia. J, Garcia. G. O, Heldwein. M. L, "Three-phase five-level active-neutral-point-clamped converters for medium voltage applications," in Power Electronics Conference (COBEP), Brazilian, 2013, pp. 85